Scientific Research Publishing

Optics and Photonics Journal, 2023, 13, 189-198
https://www.scirp.org/journal/opj
ISSN Online: 2160-889X
ISSN Print: 2160-8881

Synthesis and Conductivity Characterization of Anti-Perovskite Na_3OX Solid Electrolytes for All Solid Na-Ion Batteries

Wei Shi[1*], Masataka Ohta[1], Hiroaki Asakawa[1], Yuki Osaki[1], Mariko Murayama[1,2], Xinwei Zhao[1,3*]

[1]Department of Physics, Tokyo University of Science, Tokyo, Japan
[2]Faculty of Science and Engineering, Toyo University, Saitama, Japan
[3]International Institute for Urban Systems Engineering, Southeast University, Nanjing, China
Email: *1221707@ed.tus.ac.jp, *xwzhao@rs.tus.ac.jp

How to cite this paper: Shi, W., Ohta, M., Asakawa, H., Osaki, Y., Murayama, M. and Zhao, X.W. (2023) Synthesis and Conductivity Characterization of Anti-Perovskite Na_3OX Solid Electrolytes for All Solid Na-Ion Batteries. *Optics and Photonics Journal*, **13**, 189-198.
https://doi.org/10.4236/opj.2023.137017

Received: July 1, 2023
Accepted: July 28, 2023
Published: July 31, 2023

Abstract

Solid electrolytes for all solid sodium-ion batteries have been attracting much attention as an alternative energy storage system, which have the advantage of being extremely safe because it can be charged quickly and is nonflammable. We have synthesized anti-perovskite type Na_3OX (X = Br, and I) electrolytes with high purity, by reactions of halogen mixtures with sodium oxides. After mixing, it was filled in an alumina crucible and heated for 6 hours at 330˚C. It was confirmed that a large crystal strain was introduced by eutectication, which might reduce the activation energy of Na ion conduction and lead to an improvement of the conductivity. A relatively higher ionic conductivity of $\sigma = 1.55 \times 10^{-7}$ S/cm at 60˚C has been obtained for $Na_3OBr_{0.6}I_{0.4}$, which is about three orders higher than that in literature. A different ratio of X (X = Br, I) ions was added into sodium oxide to make the Na_3OX crystal. The influence of strain introduction on optimizing the bottleneck and improving the conductivity was discussed.

Keywords

Sodium Ion Battery, Solid Electrolyte, Ionic Conductivity, Anti-Perovskite

1. Introduction

There have been considerable attentions on secondary ion batteries due to the industry developments on computers, smartphones, and electric vehicles (EV). Lithium-ion batteries (LIB) are now the main product using in wide area [1] [2]. However, with the cost increase of LIB as well as energy resource risk and envi-

ronmental problems, sodium-ion batteries (SIB) have been attracting much attention as an alternative energy storage system in recent years [1] [2] [3]. In the research on battery with higher voltage, higher capacity and stable cycle characteristics, synthesizing various materials such as electrodes and electrolytes were important topics [4] [5] [6] [7] [8]. Since most of the commercial batteries, for both LIB and SIB, use a liquid electrolyte (LE), a solid electrolyte (SE) is necessary for achieving all solid state batteries [9] [10] [11] [12]. Comparing to LE, SE is electrically and chemically stable and has the advantage of being extremely safe because it can be charged quickly and is nonflammable. Comparing with lithium (Li), sodium (Na) has its price advantage in high volume demand for high-density and large-capacity batteries with the widespread use of EV [13] [14]. Therefore, it is urgent to improve the performance of Na-SE material (application requirement: $\sigma > 10^{-3}$ S/cm at room temperature) [15] [16], which is relatively low at present. Thus, this work is aimed on changing the composition of halogen elements to introduce additional lattice distortion and lower the ionic conduction barriers.

Compared with sorts of SE materials, Na-rich anti-perovskite SE has its unique advantages of loosening the bottleneck and increasing the ion conductivity by increasing a lattice distortion [17] [18] [19] [20]. In a Na-rich anti-perovskite structure, theoretical calculations indicated that Na_3OX (X = Cl, Br, I) materials give a relatively lower activation energy and lead to a higher conductivity, as shown in **Figure 1** [21] [22] [23].

This study aims to clarify the relationship between the structure of SE Na_3OX (X = Br, I), where changing halogen elements and their ratios, and then to improve their conductivity based on results of a structural investigation. We first synthesized the anti-perovskite type Na_3OX (X = Br, I) electrolytes. The ionic conductivity measurements indicated that the conductivity of SE Na_3OX has been improved by introducing lattice distortion. A relatively higher ionic conductivity of $\sigma = 1.55 \times 10^{-7}$ S/cm at 60˚C has been obtained for $Na_3OBr_{0.6}I_{0.4}$, which is about three orders higher than that of Na_3OBr in literature [24].

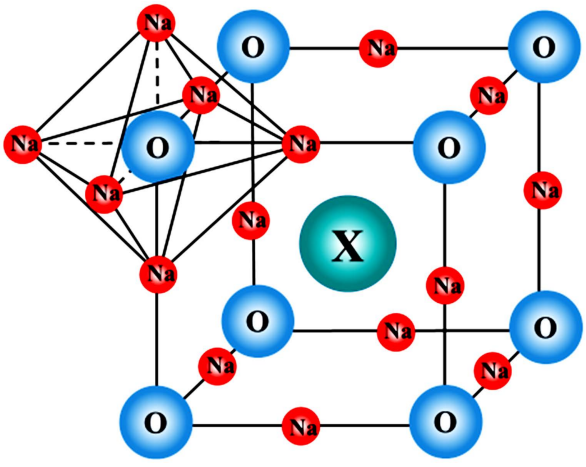

Figure 1. Crystal structure of an anti-perovskite Na_3OX (X = Cl, Br, I) lattice.

2. Experimental Methods

We added different ratio of X (X = Br, I) ions into sodium oxide to make high-purity synthetic Na_3OX crystal, then using X-ray diffraction (XRD) measurements to identify their crystal structure and material purity. And we used the Williamson-Hall analysis to evaluate the lattice distortion of the fabricated samples. Impedance measurements were carried out to analyze the ion conductivity activation energy. Scan electron microscope (SEM) and energy dispersive X-ray spectroscopy (EDS) were used to measure the surface morphology and ion distribution of the sample.

$$0.8Na_2O + 0.2Na_2O_2 + (1-x)NaBr + xNaI \rightarrow Na_3OBr_{1-x}I_x + 0.1O_2\uparrow \quad (1)$$

The Na_3OX (X = Br, I) SE materials were synthesized by above mentioned reactions. First, NaX (X = Br, I) materials were crushed and mixed in a glove box filled with N_2. Then quickly grind sodium oxide ($0.8Na_2O + 0.2Na_2O_2$) was added with the above halogen mixture. After mixing, it was filled in an alumina crucible and heated for 6 hours at 330˚C. Then, to promote the reaction, the obtained sintered body was re-crushed and reheated to obtain a pure reacting material.

XRD measurements were performed at room temperature using a system Altima IV manufactured by Rigaku, in the range of about $2\theta = 30^\circ$ to 110° in steps of 0.01˚. The ionic conductivity measurements were carried out with the equipment provided by JFE Techno Research. The crushed sample powder was placed in a measurement cell (inner diameter 10 mm) and pressed in an Ar glove box at a pressure of 2.0 tons (250 MPa) for 15 minutes to form pellets with a thickness of about 0.5 mm. The AC impedance characteristic was carried out by the sandwiched two-terminal method using a blocking electrode and evaluated with a device Bio Logic VSP. The measuring temperatures were changed from 20˚C to 60˚C in a running range of 1 to 50 MHz. The whole measurements were carried out in the same glove box to avoid the deoxidization of the samples. The Na_3OX (X = $Br_{0.8}I_{0.2}$, $Br_{0.7}I_{0.3}$, and $Br_{0.6}I_{0.4}$) samples were measured. The Na_3OBr sample was highly insulated and could not give a good result.

3. Results and Discussion

3.1. Results

Figure 2 shows the XRD measurement results of the Na_3OX samples (5 compositions in total, Na_3OBr, $Na_3OBr_{0.9}I_{0.1}$, $Na_3OBr_{0.8}I_{0.2}$, $Na_3OBr_{0.7}I_{0.3}$, and $Na_3OBr_{0.6}I_{0.4}$). It was confirmed that all compositions up to $Br_{1-x}I_x$ (x = 0 to 0.4) had the anti-perovskite structure with *Pm-3m* cubic symmetry. It is also demonstrated that the impurity peaks could hardly be confirmed, and the weight of the precursor substance with respect to Na_3OX (X = Br, I) was estimated by using the crystal structure analysis software PDXL2 based on the crystallographic information framework (CIF) and data obtained from the results of the Rietveld analysis [25], which will be described later. These results are different from the XRD pattern

reported by Wang *et al.* [13], in which a remarkable peak split was observed when compared with the measurement results of our $Br_{1-x}I_x$ (x = 0 to 0.4) eutectics. Such a peak split was attributed to be a result of vigorous segregation of two types of halogen ions because the precursor samples were not sufficiently mixed. In our sample, only when x = 0.5 was exceeded, peak split and impurity precipitation became not negligible. It is considered that segregation occurred in this case because I (iodine) exceeded the solid solution limit, which might be in the range of x = 0.4 to 0.5.

Rietveld analysis was performed for each composition using the structural analysis software EXPO2014 [26]. Currently, the only CIF data presented in major databases are X = Cl, Br, I, and $Cl_{0.5}Br_{0.5}$, all of which are cubic perovskites belonging to the symmetry *Pm-3m*. In addition, from the waveform pattern in Figure 2, it can be inferred that the symmetry of the X = $Br_{1-x}I_x$ eutectics, which is currently unknown, belongs to same cubic symmetry up to x = 0.4. Therefore, for the synthesized $Na_3OBr_{1-x}I_x$ eutectics, Rietveld analysis was performed from x = 0 to 0.4, but all fittings were performed assuming cubic symmetry *Pm-3m*. As a result, the parameters of each composition were refined, and a CIF file containing the information was obtained. According to the fitting results of Na_3OBr and $Na_3OBr_{1-x}I_x$ (x = 0 to 0.5), it was confirmed for the first time that all compositions of $Br_{1-x}I_x$ (x = 0 to 0.4) had the anti-perovskite structure with *Pm-3m* cubic symmetry.

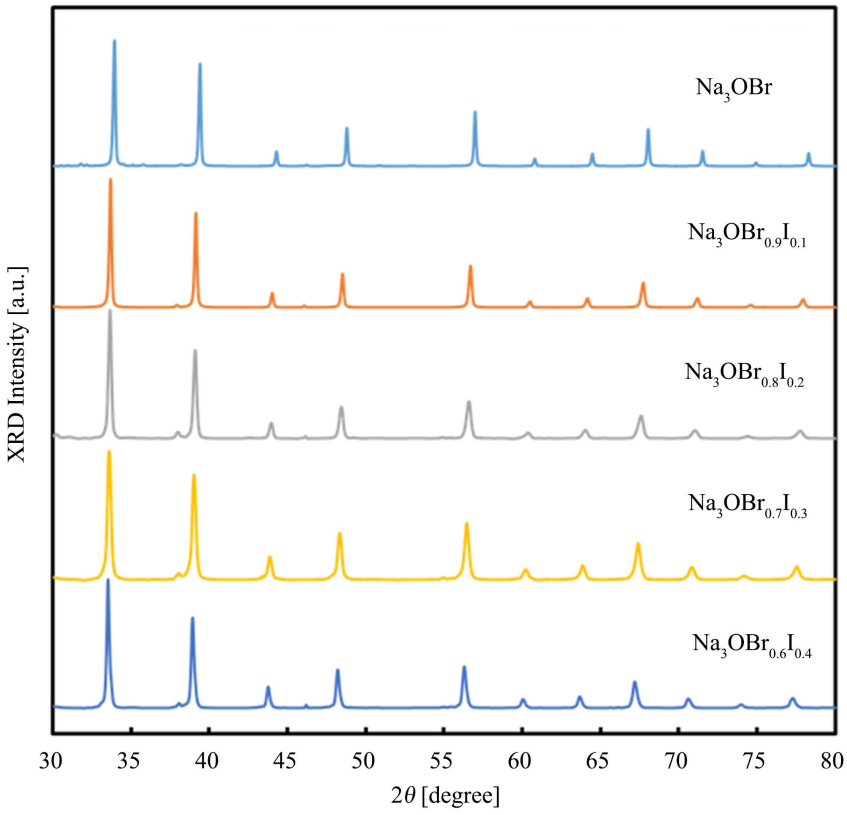

Figure 2. X-ray diffraction patterns of $Na_3OBr_{1-x}I_x$ (x = 0 to 0.4).

From the above-mentioned analysis, the crystal structure for each composition could be identified, so the counter value width was extracted for each XRD peak and Williamson-Hall (WH) plots were obtained, as shown in **Figure 3**. The half width component has been corrected by the correction formula obtained from the standard sample. The slope of the WH plots exhibits a lattice distortion ϵ, which represents a relative change of the lattice constant ($\Delta d/d$). It is clear from **Figure 3** that the introduction of significant strain was successfully achieved in the $Br_{1-x}I_x$ eutectics, which gave rise to a maximum distortion at near x = 0.2. The relative distortions comparing with Na_3OBr were ϵ = 2.3, 5.5, 4.2, and 3.4 × 10^{-3}, for $Na_3OBr_{1-x}I_x$ (x = 0.1, 0.2, 0.3, and 0.4) eutectics, respectively. These distortions might lower the activation energy (ΔEa) by loosening the bottleneck and increase the ion conductivity in the synthesized $Na_3OBr_{1-x}I_x$ eutectics. The $Na_3OBr_{0.5}I_{0.5}$ sample was not the anti-perovskite crystal structure.

Figure 4 shows the impedance results, the Cole-plots, for three $Na_3OBr_{1-x}I_x$ (x = 0.2, 0.3, and 0.4) samples measured at 60˚C. A relatively high ionic conductivity of σ = 1.55 × 10^{-7} S/cm was obtained from $Na_3OBr_{0.6}I_{0.4}$, as shown in **Figure 4**. The ionic conductivities of all samples were obtained by fitting the Cole-plots of the impedance measurements and shown in **Figure 5**. The measurement temperature was changed from 20˚C to 60˚C. Since the conductive type of SE follows the Arrhenius type, the slope of the straight line corresponds to the conductive activation energy. It is clear that the ionic conductivity of our anti-perovskite SE $Na_3OBr_{0.6}I_{0.4}$ is three orders higher than that of Na_3OBr in literature [24]. This high conductivity is considered to come from the lattice distortion caused by doping I (iodine) ions. In the impedance measurements, the resistance values of the grain boundaries and bulk had been separated using the equivalent circuit fitting software pyZwx developed by NIMS [27]. So the fitting results shown in **Figure 4** are relatively credible.

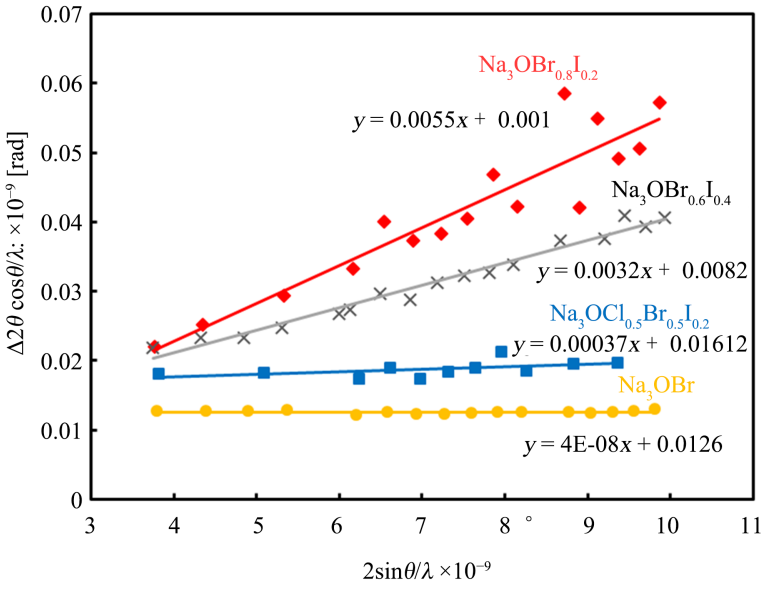

Figure 3. Williamson-Hall plots of $Na_3OBr_{1-x}I_x$ (x = 0 - 0.4).

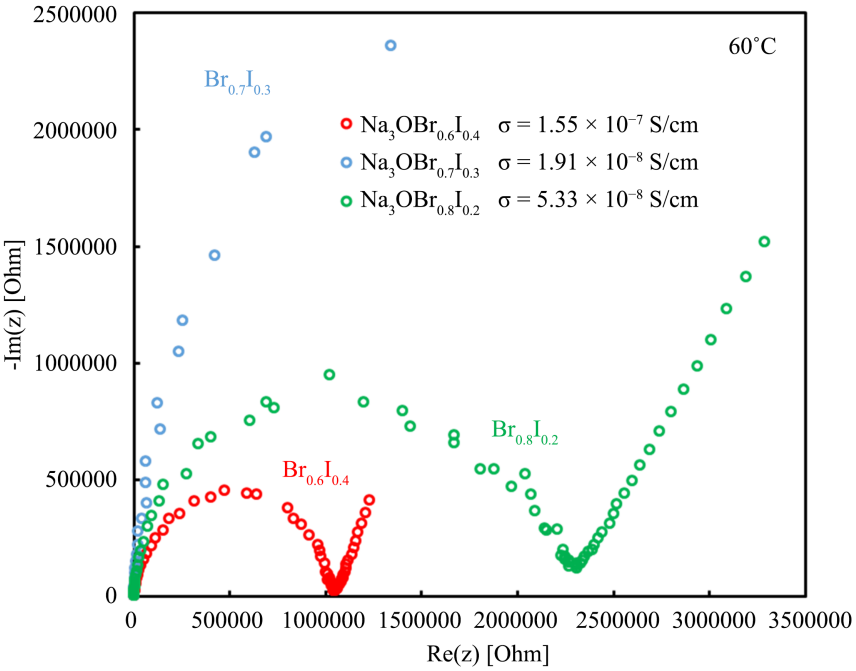

Figure 4. Cole-plots of $Na_3OBr_{1-x}I_x$ (x = 0.2 - 0.3) at 60˚C.

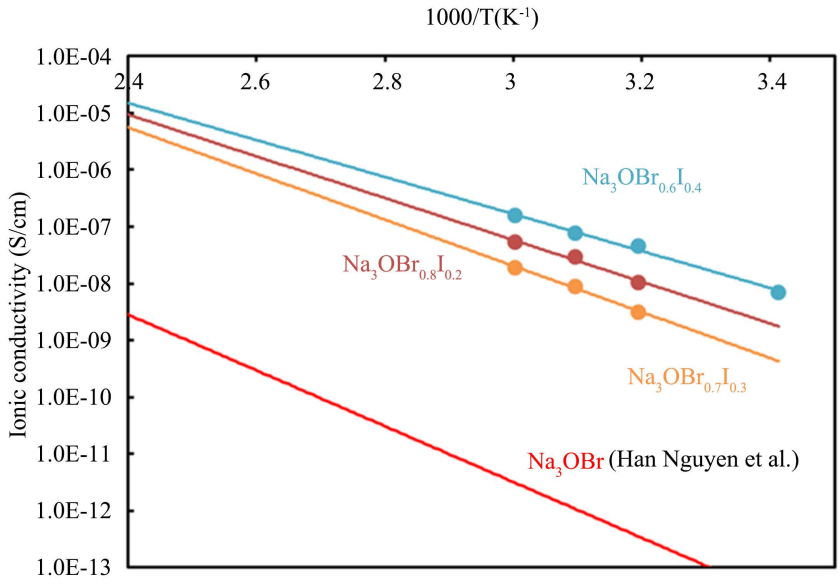

Figure 5. Arrhenius plot of ionic conductivity (σ) versus 1000/T of $Na_3OBr_{1-x}I_x$ (x = 0 - 0.4).

Furthermore, the activity energy of ionic conductivity, ΔEa, was determined by fitting the Arrhenius plots in **Figure 5**. As claimed in literature [24], ΔEa for Na_3OBr was 1.14 eV, which decreased to 0.72, 0.79, and 0.64 eV for our $Na_3OBr_{1-x}I_x$ (x = 0.2, 0.3, and 0.4), respectively. Although the activation energy did not completely decrease with the distortion increase, the bromine-iodine (B-I) mixture gave rise to the high conductivity performance by lowering the activity energy, which will be discussed below.

Since the B-I mixture played an important role in increasing ionic conductivity, the ratio of B/I and their distribution should be taken into account in the synthesis process. Figure 6 shows the surface morphology and ion distribution of Na_3OX crystals measured by SEM-EDS (Ultim Max, Oxford Instruments). Compared with pure Na_3OBr, the Br-I mixture Na_3OX got a broader eutectic. However, there was still obviously visible bromide crystal in the Br-I mixture Na_3OX surface, which might due to a lack of enough reaction time.

3.2. Discussions

A significant improvement in conductivity was observed with the $Na_3OBr_{1-x}I_x$ eutectic compared to Na_3OBr. However, the conductivity of the $Na_3OBr_{0.6}I_{0.4}$ eutectic was significantly superior to that of the $Na_3OBr_{0.8}I_{0.2}$ eutectic, even which had the largest strain. Assuming strain introduction optimizing the bottleneck as intended and destabilizing the stronger Na-O bond, a reduction in ion transfer energy and defect formation energy should be confirmed. Since the conduction activation energy is the sum of the ion transfer energy and the defect formation energy, it is considered that the conductivity reduction can be evaluated by comparing with the strain and the conductivity activation energy. It had been demonstrated that the Br-I mixture introduced additional lattice distortion in the eutectic, which led to a large reduction of the conductive activation energy from 1.14 to 0.64 eV. But the reduction of the activation energy was not completely following with the distortion increase. The reason of a rough relationship between the activation energy and the distortion was thought to be an effect of the polarizability of the introduced X ions (X: Br = 4.16, I = 6.43 [10^{-24} cm^3]) [28] [29]. When the ligand ions constituting the bottleneck are highly polar in the case of Na ion diffusing, they are flexibly deformed even if the bottleneck radius is narrow, and the Na ions could push away the ligands so that they could

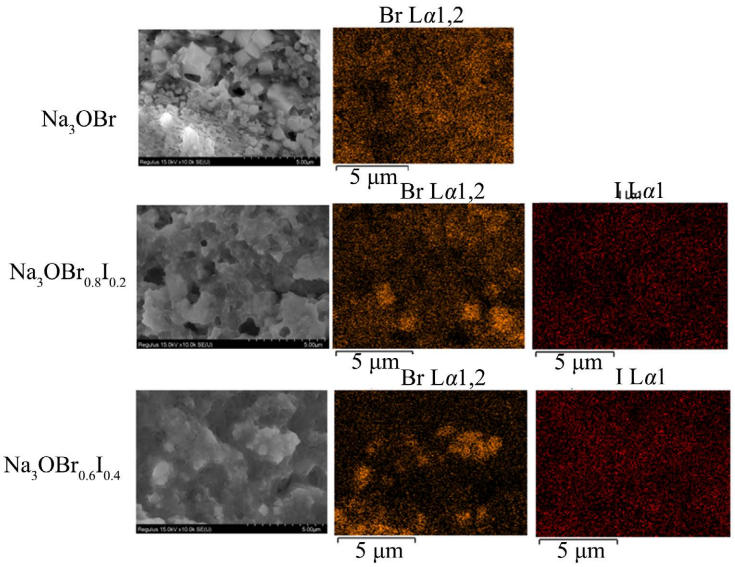

Figure 6. SEM images and EDS pictures of $Na_3OBr_{1-x}I_x$ (x = 0, 0.2, and 0.4) samples.

diffuse with low energy. From these facts, it is considered that finding a compositional balance that maximizes the contribution of both strain and polarity is an effective way to optimize the effect of improving the conductivity in the Na_3OX eutectic. It is also considered that the impedance measurement result itself changes significantly due to the influence of the surrounding environment and the pellet preparation method, which will be published next.

4. Conclusion

This research succeeded in synthesizing $Na_3OBr_{1-x}I_x$ (x = 0 to 0.4) with high purity, and confirmed that they have *Pm-3m* cubic symmetry. In addition, it was confirmed that a large crystal strain was introduced by B-I mixture eutecticization, which reduced the ion conduction activation energy, leading to the improvement of the ionic conductivity. The conductivity was maximum at $\sigma = 1.55 \times 10^{-7}$ S/cm (60˚C) for $Na_3OBr_{0.6}I_{0.4}$. A significant improvement up to several orders was achieved compared with Na_3OBr. The process optimization and high temperature measurements are in progress, which will be published later.

Acknowledgements

We would like to show our gratitude to the Dr. Guan Sujun for sharing his pearls of wisdom on the research direction, and his kindly comments and help during lab experiment that greatly improved the manuscript.

Conflicts of Interest

The authors declare no conflicts of interest regarding the publication of this paper.

References

[1] Shacklette, L.W., Toth, J.E. and Elsenbaumer, R.L. (1985) Conjugated Polymer as Substrate for the Plating of Alkali Metal in a Nonaqueous Secondary Battery. Allied Corp., Morristown.

[2] Shishikura, T. and Takeuchi, M. (1987) Secondary Batteries. Showa Denko K. K. Hitachi, Ltd., Tokyo.

[3] Kubota, K. and Komaba, S. (2015) Review—Practical Issues and Future Perspective for Na-Ion Batteries. *Journal of the Electrochemical Society*, **162**, A2538-A2550. https://doi.org/10.1149/2.0151514jes

[4] Thomas, P., Ghanbaja, J. and Billaud, D. (1999) Electrochemical Insertion of Sodium in Pitch-Based Carbon Fibres in Comparison with Graphite in $NaClO_4$-Ethylene Carbonate Electrolyte. *Electrochimica Acta*, **45**, 423-430. https://doi.org/10.1016/S0013-4686(99)00276-5

[5] Stevens, D.A. and Dahn, J.R. (2000) An *in Situ* Small-Angle X-Ray Scattering Study of Sodium Insertion into a Nanoporous Carbon Anode Material within an Operating Electrochemical Cell. *Journal of the Electrochemical Society*, **147**, 4428-4431. https://doi.org/10.1149/1.1394081

[6] Stevens, D.A. and Dahn, J.R. (2001) The Mechanisms of Lithium and Sodium Insertion in Carbon Materials. *Journal of the Electrochemical Society*, **148**, A803-A811.

https://doi.org/10.1149/1.1379565

[7] Joncourt, L., *et al.* (1996) Sodium Reactivity with Carbons. *Journal of Physics and Chemistry of Solids*, **57**, 877-882. https://doi.org/10.1016/0022-3697(95)00366-5

[8] Xia, X. and Dahn, J.R. (2012) Study of the Reactivity of Na/Hard Carbon with Different Solvents and Electrolytes. *Journal of the Electrochemical Society*, **159**, A515-A519. https://doi.org/10.1149/2.jes111637

[9] Palomares, V., *et al.* (2012) Na-Ion Batteries, Recent Advances and Present Challenges to Become Low Cost Energy Storage Systems. *Energy & Environmental Science*, **5**, 5884-5901. https://doi.org/10.1039/c2ee02781j

[10] Hwang, J.-Y., Myung, S.-T. and Sun, Y.-K. (2017) Sodium-Ion Batteries: Present and Future. *Chemical Society Reviews*, **46**, 3529-3614. https://doi.org/10.1039/C6CS00776G

[11] Slater, M.D., Kim, D., Lee, E. and Johnson, C.S. (2013) Sodium-Ion Batteries. *Advanced Functional Materials*, **23**, 947-958. https://doi.org/10.1002/adfm.201200691

[12] Yabuuchi, N., Kubota, K., Dahbi, M. and Komaba, S. (2014) Research Development on Sodium-Ion Batteries. *Chemical Reviews*, **114**, 11636-11682. https://doi.org/10.1021/cr500192f

[13] Wang, Y., *et al.* (2015) Structural Manipulation Approaches towards Enhanced Sodium Ionic Conductivity in Na-Rich Antiperovskites. *Journal of Power Sources*, **293**, 735-740. https://doi.org/10.1016/j.jpowsour.2015.06.002

[14] Sun, Y., *et al.* (2019) Rotational Cluster Anion Enabling Superionic Conductivity in Sodium-Rich Antiperovskite Na_3OBH_4. *Journal of the American Chemical Society*, **141**, 5640-5644. https://doi.org/10.1021/jacs.9b01746

[15] Gao, S., Broux, T., Fujii, S., *et al.* (2021) Hydride-Based Antiperovskites with Soft Anionic Sublattices as Fast Alkali Ionic Conductors. *Nature Communications*, **12**, Article No. 201. https://doi.org/10.1038/s41467-020-20370-2

[16] Dawson, J.A., Chen, H. and Islam, M.S. (2018) Composition Screening of Lithium- and Sodium-Rich Anti-Perovskites for Fast-Conducting Solid Electrolytes. *The Journal of Physical Chemistry C*, **122**, 23978-23984. https://doi.org/10.1021/acs.jpcc.8b08208

[17] Hasa, I., *et al.* (2021) Challenges of Today for Na-Based Batteries of the Future: From Materials to Cell Metrics. *Journal of Power Sources*, **482**, Article ID: 228872. https://doi.org/10.1016/j.jpowsour.2020.228872

[18] Ma, Q.L. and Tietz, F. (2020) Solid-State Electrolyte Materials for Sodium Batteries: Towards Practical Applications. *ChemElectroChem*, **7**, 2693-2713. https://doi.org/10.1002/celc.202000164

[19] Zhao, C., Liu, L., Qi, X., Lu, Y., Wu, F., Zhao, J., Yu, Y., Hu, Y. and Chen, L. (2018) Solid-State Sodium Batteries. *Advanced Energy Materials*, **8**, Article ID: 1703012. https://doi.org/10.1002/aenm.201703012

[20] Dawson, J.A., Famprikis, T. and Johnston, K.E. (2021) Anti-Perovskites for Solid-State Batteries: Recent Developments, Current Challenges and Future Prospects. *Journal of Materials Chemistry A*, **9**, 18746-18772. https://doi.org/10.1039/D1TA03680G

[21] Zheng, X., *et al.* (2022) Theoretical Design of Na-Rich Anti-Perovskite as Solid Electrolyte: The Effect of Cluster Anion in Stability and Ionic Conductivity. *Journal of Solid State Chemistry*, **316**, Article ID: 123643. https://doi.org/10.1016/j.jssc.2022.123643

[22] Asakawa, H., *et al.* (2022) Structural Manipulation for Solid Electrolyte Na_3OBr by

Sulfur Ions Doping. *Japanese Journal of Applied Physics*, **61**, SD1008. https://doi.org/10.35848/1347-4065/ac4e4b

[23] Li, H.X., Zhou, X.Y., Wang, Y.C. and Jiang, H. (2021) Theoretical Study of Na^+ Transport in the Solid-State Electrolyte Na_3OBr Based on Deep Potential Molecular Dynamics. *Inorganic Chemistry Frontiers*, **8**, 425-432. https://doi.org/10.1039/D0QI00921K

[24] Nguyen, H., *et al.* (2016) Experimental and Computational Evaluation of a Sodium-Rich Anti-Perovskite for Solid State Electrolytes. *Journal of the Electrochemical Society*, **163**, A2165-A2171. https://doi.org/10.1149/2.0091610jes

[25] Nakai, I. and Izumi, F. (2002) X-Ray Diffraction of Powder Materials: Introduction of Rietveld Analysis. Asakura Books. (In Japanese)

[26] Altomare, A., *et al.* (2013) EXPO2013: A Kit of Tools for Phasing Crystal Structures from Powder Data. *Journal of Applied Crystallography*, **46**, 1231-1235. https://doi.org/10.1107/S0021889813013113

[27] Kobayashi, K. and Suzuki, T.S. (2021) Free Analysis and Visualization Programs for Electrochemical Impedance Spectroscopy Coded in Python. *Electrochemistry*, **89**, 218-222. https://doi.org/10.5796/electrochemistry.21-00010

[28] Ahiavi, E., Dawson, J.A., Kudu, U., *et al.* (2020) Mechanochemical Synthesis and Ion Transport Properties of Na_3OX (X = Cl, Br, I and BH_4) Antiperovskite Solid Electrolytes. *Journal of Power Sources*, **471**, Article ID: 228489. https://doi.org/10.1016/j.jpowsour.2020.228489

[29] Kim, K. and Siegel, D.J. (2019) Correlating Lattice Distortions, Ion Migration Barriers, and Stability in Solid Electrolytes. *Journal of Materials Chemistry A*, **7**, 3216-3227. https://doi.org/10.1039/C8TA10989C